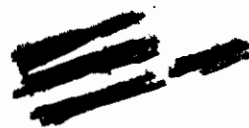


*Contrails*

AN APPROXIMATE SOLUTION  
OF UNSTEADY TRANSONIC FLOW PROBLEMS

J. M. WU

K. R. KIMBLE



APPROVED FOR PUBLIC RELEASE; DISTRIBUTION UNLIMITED

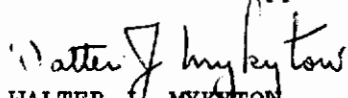
## FOREWORD

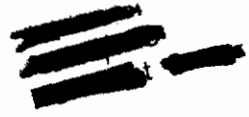
The research described in this report was performed by The University of Tennessee Space Institute, Tullahoma, Tennessee, for the Aerospace Dynamics Branch, Vehicle Dynamics Division, Air Force Flight Dynamics Laboratory, Wright-Patterson Air Force Base, Ohio, under Contract F33615-73-C-3119, Project No. 1929, "Research in Flight Vehicle Dynamics", Task No. 192905, "Transonic Unsteady Aerodynamics". The project monitor was Mr. James J. Olsen of the Design Analysis Group.

The work reported herein was conducted during the period of June 15, 1973 through January 15, 1974. The Principal Investigator was Jain-Ming (James) Wu, who was assisted by Kenneth R. Kimble.

The manuscript was released by the authors for publication on 20 February 1974.

This technical report has been reviewed and is approved.

  
WALTER J. MYKUTOW  
Asst. for Research & Technology  
Vehicle Dynamics Division



ABSTRACT

Unsteady pressures on a thin two-dimensional airfoil pitching and plunging in transonic flow have been computed by numerically solving the governing partial differential equation. The effect of wing thickness has been retained by using the steady flow potential on the wing in the coefficients of the equation in a manner which generalizes Oswatitsch's parabolic method. The results are compared with other methods and with experimental data.

## TABLE OF CONTENTS

SECTION		PAGE
I	INTRODUCTION	1
II	TECHNICAL DISCUSSION	3
	1. Statement of Problem	3
	2. Parabolic Method	5
	3. Present Method	7
III	RESULTS	9
	1. Teipel's Parabolic Method	9
	2. Spreiter-Stahara's Local Linearization Method	9
	3. Parabolic Arc Airfoil	9
	4. Control Surface Oscillation	10
IV	CONCLUSIONS AND RECOMMENDATIONS	12
	REFERENCES	28

## LIST OF ILLUSTRATIONS

Figure	Title
1.	Pressure distribution for a parabolic arc profile (plunging, $M_\infty = 1.0$ ). Analytic results due to Teipel.
2.	Real part of unsteady pressure coefficient for pitching wing.
3.	Imaginary part of unsteady pressure coefficient for pitching wing.
4.	Magnitude of unsteady pressure distribution on 6% parabolic arc airfoil oscillating in plunge at $M_\infty = 1$ .
5.	Phase of unsteady pressure distribution on 6% parabolic arc airfoil oscillating in plunge at $M_\infty = 1$ .
6.	Magnitude of unsteady pressure distributions on 6% parabolic arc airfoil pitching about the nose at $M_\infty = 1$ .
7.	Phase of unsteady pressure distributions on 6% parabolic arc airfoil pitching about the nose at $M_\infty = 1$ .
8.	6% parabolic airfoil oscillating in plunge.
9.	6% parabolic airfoil pitching about the nose.
10.	Oscillating control surface for $M_\infty = .944$ at reduced frequency $k = .220$ .
11.	Oscillating control surface for $M_\infty = .961$ at reduced frequency $k = .163$ .
12.	Oscillating control surface for $M_\infty = .964$ at reduced frequency $k = .216$ .
13.	Oscillating control surface for $M_\infty = .966$ at reduced frequency $k = .054$ .
14.	Oscillating control surface for $M_\infty = .984$ at reduced frequency $k = .212$ .
15.	Oscillating control surface for $M_\infty = .994$ at reduced frequency $k = .211$ .

## LIST OF SYMBOLS

$a_{\infty}$	Free stream speed of sound
$b$	Wing chord
$C_n$	Equation 23
$C_p$	Steady pressure coefficient
$\bar{C}_p$	Equation 22
$\tilde{C}_p$	Unsteady pressure coefficient (real part)
$\tilde{C}_p^{\text{im}}$	Unsteady pressure coefficient (imaginary part)
$D_n$	Equation 26
$f$	Body thickness distribution
$g$	Body displacement distribution
$k$	Reduced frequency
$M_{\infty}$	Free stream Mach number
$\rho^n$	Equation 24
$t$	Time
$U_0$	Free stream velocity
$U, V$	Local velocities
$x, y$	Spatial coordinates

# Contrails

$z_{\infty}$	Numeric infinity in $\eta$ direction
$\gamma$	Specific heat ratio
$\Gamma$	Parabolic constant
$\delta$	Magnitude of unsteady displacement
$\delta_{\eta}$	Central difference operator in $\eta$ direction
$\epsilon$	Thickness ratio
$\eta$	Non-dimensionalized y coordinate
$\bar{\eta}$	Stretched $\eta$ coordinate
$\xi$	Non-dimensionalized x coordinate
$\bar{\xi}$	Stretched $\xi$ coordinate
$\phi$	Velocity potential
$\phi$	Steady velocity potential
$\bar{\phi}$	Spreiter's similarity steady velocity potential
$\phi$	Unsteady velocity potential
$\Psi$	Non-dimensionalized velocity potential
$\omega$	Oscillation frequency
$\tau$	Non-dimensionalized time

# *Contrails*



# Contrails

## SECTION I

### INTRODUCTION

The fundamental difficulty in the study of transonic flow is due to the presence of interaction of advancing and receding dispersive waves which results in the well-known Riemann steepening of the wave fronts [1]\* at sonic speeds. This phenomenon is reflected even in the first approximation equations of small perturbation theory by the presence of a non-linear term in the governing equation. The resulting non-linear equation of mixed type is further complicated by the fact that the sonic line along which the type changes is determined by the solution and is not available a priori.

The solution to the non-linear steady equation may be accomplished by finite difference techniques or by various heuristic approximation methods [2]. Only recently have finite difference techniques been improved sufficiently to solve the two-dimensional and axisymmetric body non-linear equations with sufficient accuracy in a reasonable time [for instance, 3]. Progress has also been made in solving the three-dimensional problem [4]. However, these are very time consuming methods and if repeated several times, as would be necessary for unsteady calculations over a range of frequencies and for a variety of oscillation modes, would become prohibitively costly [5, pp. 10-13].

By treating unsteady motion as a small perturbation of steady motion, one may split the total unsteady flow into two parts as was done by Landahl [6]. For large frequencies or very slender bodies, Landahl showed that the two parts were decoupled and thus was able to solve the unsteady problem without solving the steady problem. Liu, Platzler, and Ruo [7] and Kimble, Ruo, Liu and Wu [8] have extended this method for bodies of revolution and pointed slender wings (hence, a limited three-dimensional geometry) to include a first approximation to the effect of the steady solution by the use of the parabolic method.

The above solutions as well as that of Teipel [9] for the two-dimensional case have been given in asymptotic form. This is not wholly satisfactory since the series are not uniformly valid near the nose or leading edge.

Also the asymptotic methods are impractical if the influence of the steady part is approximated more realistically by a function which varies with position in the flow field rather than by the parabolic constant [see 2].

---

\*Numbers quoted in brackets are references cited at the end of the report.

# *Contrails*

A numeric procedure has been devised to solve the unsteady equation very rapidly for Mach number near one. It takes advantage of the extent of the sonic pocket in such flows resulting in an equation of parabolic and hyperbolic type near the body.

Solutions were obtained for the pitching and plunging parabolic arc airfoil as well as the oscillating control surface problem for which Tijdeman and Bergh [10] obtained experimental solutions. The theoretical solutions are quantitatively similar to those of Tijdeman and Bergh but show much smoother trends. This discrepancy and its possible causes are discussed in the conclusions.

SECTION II

TECHNICAL DISCUSSION

1. Statement of Problem

Assuming a uniform two-dimensional flow of velocity  $U_0$  directed in the positive x direction for points far upstream and a thin body of length b oriented mainly along the x axis with leading edge at  $x = 0$  and executing small transverse vibrations it is permissible to assume that the flow has a velocity potential  $\phi$  such that

$$U = U_0 (1 + \bar{\Phi}_x) , \quad V = U_0 \bar{\Phi}_y \quad (1)$$

where U and V are the velocity components in the x and y directions respectively. It has been shown, e.g. [6], that the small perturbation assumptions give

$$[1 - M_\infty^2 - M_\infty^2(\gamma + 1)\bar{\Phi}_x] \bar{\Phi}_{xx} + \bar{\Phi}_{yy} - 2M_\infty^2 \bar{\Phi}_{xt}/a_\infty - \bar{\Phi}_{tt}/a_\infty^2 = 0 \quad (2)$$

for the equation to be satisfied by  $\phi$  in the first approximation for small thickness. Here  $M_\infty$  is the Mach number at upstream infinity,  $\gamma$  is the ratio of specific heats, and  $a_\infty$  is the sonic velocity for upstream. After the change of variables

$$x = b\xi , \quad y = b\eta , \quad t = b\tau/U_0 , \quad \bar{\Phi} = b\bar{\Psi} \quad (3)$$

the potential equation becomes

$$[1 - M_\infty^2 - M_\infty^2(\gamma + 1)] \bar{\Psi}_{\xi\xi} + \bar{\Psi}_{\eta\eta} - 2M_\infty^2 \bar{\Psi}_{\xi\tau} - M_\infty^2 \bar{\Psi}_{\tau\tau} = 0 \quad (4)$$

Further,  $\bar{\Psi}$  must approach zero far upstream and at large lateral distances from the body. The condition of tangential flow on the body gives

# Contrails

$$\Psi_{\eta} ]_{body} = H_{\xi} + H_{\tau} \quad (5)$$

where  $\eta = H(\xi, \tau)$  for points on the body and where the body is assumed to be thin. The body may be described by

$$H(\xi, \tau) = \epsilon g(\xi) + \delta \text{Real}(f(\xi) e^{ik\tau}) \quad (6)$$

where  $\epsilon$  is the thickness ratio and  $\delta$  represents the oscillation amplitude at reduced frequency  $k = \omega b/U_0$  ( $\omega$  is the frequency while  $g(\xi)$  and  $f(\xi)$  both of order 1, are the distributions of thickness and "oscillation amplitude", respectively.)

Then writing

$$\Psi(\xi, \eta, \tau) \equiv \phi(\xi, \eta) + \text{Real}\{\varphi(\xi, \eta) e^{ik\tau}\} \quad (7)$$

and assuming

$$[1 - M_{\infty}^2 - M_{\infty}^2(\gamma + 1)\phi_{\xi\xi}] \phi_{\xi\xi} + \phi_{\eta\eta} = 0 \quad (8)$$

and

$$\phi_{\eta} ]_{body} = \epsilon g(\xi) \quad (9)$$

we have [6, p.7],

$$\begin{aligned} (1 - M_{\infty}^2) \varphi_{\xi\xi} - M_{\infty}^2(\gamma + 1) (\phi_{\xi} \varphi_{\xi\xi} + \phi_{\xi\xi} \varphi_{\xi}) \\ + \varphi_{\eta\eta} - 2M_{\infty}^2 ik \varphi_{\xi} + M_{\infty}^2 k^2 \varphi = 0 \end{aligned} \quad (10)$$

and assuming the thickness ratio  $\epsilon$  is small, the condition of tangential flow becomes

# Contrails

$$\varphi_{\eta}(\xi, \pm 0) = \delta(f_{\xi} + ikf), \quad 0 < \xi < 1 \quad (11)$$

Defining  $\varphi^*(\xi, \eta) = \varphi(\xi, -\eta)$  we see that  $\varphi^*$  satisfies the same differential equation and boundary conditions as  $\varphi$  except that

$$\varphi_{\xi}^*(\xi, +0) = -\delta(f_{\xi} + ikf) = -\varphi_{\xi}(\xi, +0) \quad (12)$$

Therefore, the uniqueness of the solution of the problem implies that

$$\varphi(\xi, -\eta) = \varphi^*(\xi, \eta) = -\varphi(\xi, \eta) \quad (13)$$

and setting  $\eta = 0$  gives

$$\varphi(\xi, 0) = 0, \quad -\infty < \xi \leq 0 \quad \text{or} \quad 1 \leq \xi < \infty \quad (14)$$

Pressure coefficients may be computed for steady flow from

$$C_p \equiv -2\phi_{\xi} \quad (15)$$

and for unsteady flow from

$$\tilde{C}_p + i\tilde{C}_p \equiv -2(\varphi_{\xi} + ik\varphi) \quad (16)$$

## 2. Parabolic Method

Equation 10 is a variable coefficient linear equation which requires knowledge of the steady flow potential for its solution. Oswatitsch [11] and Cole and Royce [12] have used simplified representations of  $\phi_{\xi}$  for  $M_{\infty}$  very near 1 with great success to predict pressures on the body. The principal argument is that the sonic pocket is very extensive in the y direction and extends nearly the whole length of the body. Hence the flow near the body is largely supersonic and the governing equations (8) and (10) are hyperbolic. The extent of the pocket prevents much

# Contrails

feedback from the wake into the solution in the elliptic region ahead of the body. In addition, little upstream influence is generated by the body owing to the nearness of  $M_\infty$  to 1.

Cole used an approximation which allowed for the hyperbolic behavior of the equation (8):

$$\phi_x = (x - x^*) C, \quad \phi_{xx} = -C \quad (17)$$

where  $x^*$  is the sonic point and  $c$  is a positive constant. Oswatitsch used the fact that the characteristics are extremely steep inside the pocket and concluded that the equation would exhibit a nearly parabolic behavior inside the pocket. Oswatitsch took advantage of this behavior by assuming  $\phi_{\xi\xi}$  was a positive constant, the parabolic constant  $\Gamma$ , hence giving a parabolic equation

$$\left[ 1 - M_\infty^2 - M_\infty^2 (\gamma + 1) \phi_\xi \right] \Gamma + \phi_{\eta\eta} = 0 \quad (18)$$

for  $\phi$ . The behavior of this equation (as well as that of Cole) is consistent with the above observations. The potential may be assumed zero at the leading edge of the body and the solution is then computed within the sonic pocket and is independent of wake and upstream influence.

Various methods of assigning values to  $\Gamma$  and of improving these approximations by allowing  $\Gamma$  to change with  $\xi$  have been developed by Spreiter [13], Wu [1], Hosokawa [14], Teipel [9], Zierep [15] and others. Platzler [16], Liu and Ruo [17] and Kimble, et al [8] have calculated asymptotic solutions of (10) using

$$\phi_\xi = 0, \quad \phi_{\xi\xi} = \Gamma \quad (19)$$

and Spreiter and Stahara [18] have included Spreiter's local linearization solution for  $\phi$  in a solution for the two-dimensional case. For comparison purposes we have chosen the work of Teipel [9] in which the constant  $\Gamma$  is given by

$$\phi_{\xi\xi} \cong \Gamma = 1.559 [(\gamma + 1) \epsilon]^{2/3}, \quad \phi_\xi = 0 \quad (20)$$

and the work of Spreiter and Stahara in which

$$\begin{aligned} \bar{\phi}_\xi &= \left[ \frac{12}{\pi} \left\{ \ln(4\xi) - 8\xi + 8\xi^2 + \frac{3}{2} \right\} \right]^{1/3} \\ \bar{\phi}_{\xi\xi} &= \frac{2}{2\xi} \bar{\phi}_\xi \end{aligned} \quad (21)$$



# Contrails

where

$$\bar{\phi}(\xi, \eta) = \phi(\xi, \eta [M_\infty^2(\gamma+1)\epsilon]^{-1/3}) \left[ \frac{\epsilon^2}{M_\infty^2(\gamma+1)} \right]^{-1/3}$$
$$C_p = \left[ \frac{\epsilon^2}{M_\infty^2(\gamma+1)} \right]^{1/3} \bar{C}_p \quad (22)$$

### 3. Present Method

The parabolic method gives good agreement with experiments for values of the generalized force coefficients (total-damping-in-pitch). These coefficients represent an "average" of the flow effects over the entire body and hence it is not so surprising that the simplified representation of the steady flow provides reasonably good approximation for their values.

However, in order to represent the unsteady pressure distributions on the body accurately, more detailed descriptions of the steady solution values on the body must be used.

Since experimental results generally include measurement of the steady flow conditions, the method should be able to accept these results as input in order to calculate the unsteady conditions. Also, many numeric solutions have even been obtained for the steady case. It should be possible to use these as well.

The only method of solution of equation (10) which can accept such data as input is a numeric method. Consequently, a numeric solution procedure similar to that of Crank-Nicolson was used to solve equation (10).

The steady flow ahead of the body is assumed to have no effect. The solution is computed to the hyperbolic equation (10) forward from the leading edge along the x axis until  $\phi_\xi \leq 0$ . This is the point at which the steady flow shock is encountered. Since near  $M_\infty = 1$ , the shock is near the trailing edge, computation is terminated.

The  $\xi$  derivative terms are approximated by a difference scheme which gives good accuracy and stability regardless whether equation (10) is hyperbolic or parabolic and makes the comparison of the various methods more convenient. Let

$$C_{n+1/2} \equiv M_\infty^2(\gamma+1) \phi_{\xi\xi} \left( (n+1/2)\Delta\xi, 0 \right) \quad (23)$$

# Contrails

Denote by  $\delta_\eta$  the central difference operator in the  $\eta$  direction and by  $\left[ \cdot \right]_{n, n+1}$  to evaluate at  $n$  and  $n+1$  and add as opposed to the usual meaning of  $\left[ \cdot \right]_{n+1}$ . Then the basic difference equation for the parabolic method is

$$\mathcal{P}^{n+1/2} [\varphi_i] \equiv C_{n+1/2} [\varphi_i]_n^{n+1} - \frac{\Delta \xi}{2\Delta \eta^2} \left[ \delta_\eta^2 \varphi_i + M_\infty^2 k^2 \varphi_i \right]^{n, n+1} = 0 \quad (24)$$

From this we may define the scheme for the hyperbolic equation as

$$D_n \delta_\xi^2 \varphi_i^n + \Delta \xi \frac{1}{2} \left[ \mathcal{P}^{n+1/2} [\varphi_i] + \mathcal{P}^{n-1/2} [\varphi_i] \right] = 0 \quad (25)$$

where

$$D_n = (1 - M_\infty^2) - M_\infty^2 (\gamma + 1) \phi_\xi (n \Delta \xi, 0) \quad (26)$$

This scheme has the advantage of retaining truncation error  $\mathcal{O}(\Delta \xi^2 + \Delta \eta^2)$  for either hyperbolic or parabolic methods. It is unconditionally stable and we believe takes full advantage of the fact that the equation (10) is actually nearly parabolic, a fact which is reflected in the small magnitude of the coefficient  $D$ .

In addition (and before differencing) the equation was transformed so as to give a finite region of solution. The transformation is

$$\eta = \frac{2}{\pi} \tan \left( \frac{\pi}{2} \bar{\eta} \right) \quad (27)$$

By this means the boundary condition at  $\eta = \infty$  becomes a condition at  $\bar{\eta} = 1$ , making consideration of far field solutions unnecessary.



## SECTION III

### RESULTS

#### 1. Teipel' s Parabolic Method

Calculations were first carried out according to Teipel's procedure since in that case an analytic solution may be obtained and an appraisal of the error in the numeric method obtained. Figures 1 - 3 show that the error is less than 1% except near the nose singularity. Various values of  $z_\infty$ , the value of  $\eta$  beyond which the solution is assumed zero, were used and it was found that only at  $z_\infty = 8$  was the influence of the far field negligible. This gives some idea of the persistence of the unsteady flow far from the body. The transformation (22) decreased greatly the number of  $\eta$  points necessary to obtain an accurate solution. The values of pressure coefficient differed by less than 2% from those for case for  $z_\infty = 8$ . Note that the wing occupies the region  $-1 \leq x \leq 1$  on the  $x$  scale. Here  $x = 2\xi - \frac{1}{2}$ . This is done in agreement with Teipel's paper in which also  $C_p$ ,  $\tilde{C}_p$  represent the real and imaginary parts of the unsteady pressure.

#### 2. Spreiter-Stahara's Local Linearization Method

The steady flow solution of Spreiter-Stahara was used in the present program to predict the unsteady potential and the results compared in Figures 4 - 7 with the local linearization method of solving the same equation. As reduced frequency  $k$  increases both solutions approach that of slender body theory as they should. However differences on the order of 50% occur as  $k$  is reduced to .1. In both methods, the steady flow is assumed independent of  $\eta$ ; in both methods no influence of flow ahead of the body nor shock nor wake influence is assumed. In short, both solve the same mathematical problem. No mathematical justification has been given for the local linearization method; however, the numeric method has been well studied. We conclude that the local linearization method is not sufficiently accurate to be used for values of reduced frequency near .1.

#### 3. Parabolic Arc Airfoil

The present method was used to compute the unsteady pressures which result when a parabolic arc airfoil is oscillating in pitch or in plunge at reduced frequency  $k = .1$ . The steady data was taken from the experimental results of Knechtel [21, fig. 7] for a low Mach number of  $M_\infty = .806$  and a Mach number near 1 of  $M_\infty = 1.083$ . The results are shown in figures 8 and 9. It was not expected that the present method would yield results beyond  $x = .9$  for  $M_\infty = .806$  since the equation is no longer hyperbolic there. Some difficulty is experienced even before

this, however. The coefficient of  $\varphi_{\xi\xi}$  is quite small and hence when the real coefficient of  $\varphi_{\xi}$  becomes negative ( $x > .5$ ) the solution is rather inaccurate.

However near the leading edge only the parabolic equation is used and consequently no difficulty with instability is encountered.

Some inaccuracy is also due to the use of rather crude interpolation of the experimental data. It would be much better to use a parabolic interpolation rather than the linear interpolation used here.

#### 4. Control Surface Oscillation

The only experimental data available to us are the experiments of Tijdeman and Bergh [10]. Although these are not really satisfactory tests of the present method, an attempt was made to determine whether reasonable results could be obtained. The values of  $\delta_{\xi}$  and  $\delta_{\xi\xi}$  were derived from the steady data given in [19, fig. 2] for  $M_{\infty} = .94, .96, .98, 1.00$ . These were used for computing the unsteady pressures as shown in figures 10 - 15.

There is agreement between experimental and theoretical results only in order of magnitude. The present method cannot predict unsteady flow pressures behind the shock and hence the graph has been terminated ahead of the shock position. Interestingly the experimental data confirm the assumption that the flow is only slightly affected ahead of the oscillating surface for Mach number near 1. Thus in figure 10 of reference 19 pressures are virtually zero ahead of  $x/c = .75$  for  $M_{\infty} = .984, .994$ .

We feel that the experimental data must be viewed with great care, however. There is not sufficient investigation of the repeatability of the experiments. Although repeated runs were made to measure aerodynamic derivatives and these did show consistency, it is well known that most theories, even fully linearized ones, give rather good predictions of the aerodynamic derivatives. These derivatives are actually integrals of the pressure over the body and tend to average out many errors present. We are concerned that the unsteady pressure changes by more than 50% from one  $x$  station to the next, in several cases, particularly when  $M_{\infty}$  is near 1.0. Additional tests should be made to determine whether these data are repeatable.

The wind tunnel-model combination has a blockage ratio of 2%. Other investigators [20] have established that steady transonic flow requires a ratio of less than 1% to alleviate wind tunnel wall effects. These effects are worst near the trailing edge where the reflected wave from the tunnel wall strikes the airfoil. Unsteady flow perturbations would seem to extend

# *Contrails*

even further in the lateral direction than do the steady effects. This may well account for the sharp variations in the experimental data.

## SECTION IV

### CONCLUSIONS AND RECOMMENDATIONS

The numeric method presented here has been shown to be more versatile and in some cases more accurate than other methods which ignore the elliptic part of the flow field. At the same time, the importance of including wake effect, particularly for oscillating control surfaces is evident. The present method is quite fast requiring less than 30 seconds per case on the IBM 360/65. The method could be modified to include wake influence at a fraction the cost of a full solution of the mixed type equation (10). The effect of more accurately modelling the steady flow by using a damping factor for its value in the  $\eta$  direction should be investigated.

Perhaps the most important recommendation which can be made is to the need of experimental data. Most theoretical work done at present has only limited application to the Tijdeman-Bergh experiments where shock influence, wake influence, and tunnel wall effects are most severe. Only by comparison with experiments in which the entire surface oscillates will it be possible to sufficiently separate these effects to determine how they cumulatively affect the current situation.

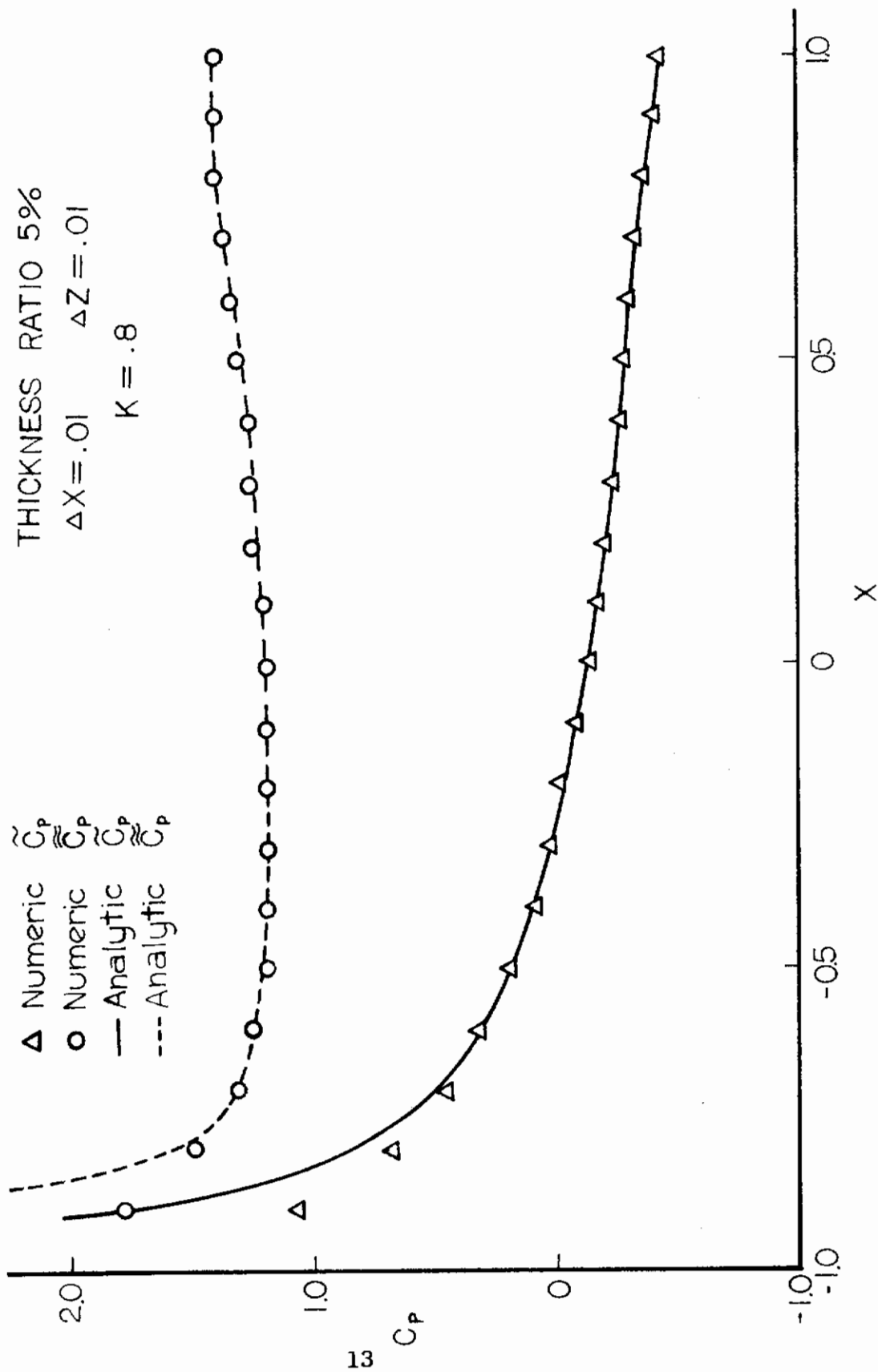


Figure 1. Pressure distribution for a parabolic arc profile. (plunging,  $M_\infty = 1.0$ ). Analytic results due to Teipel.

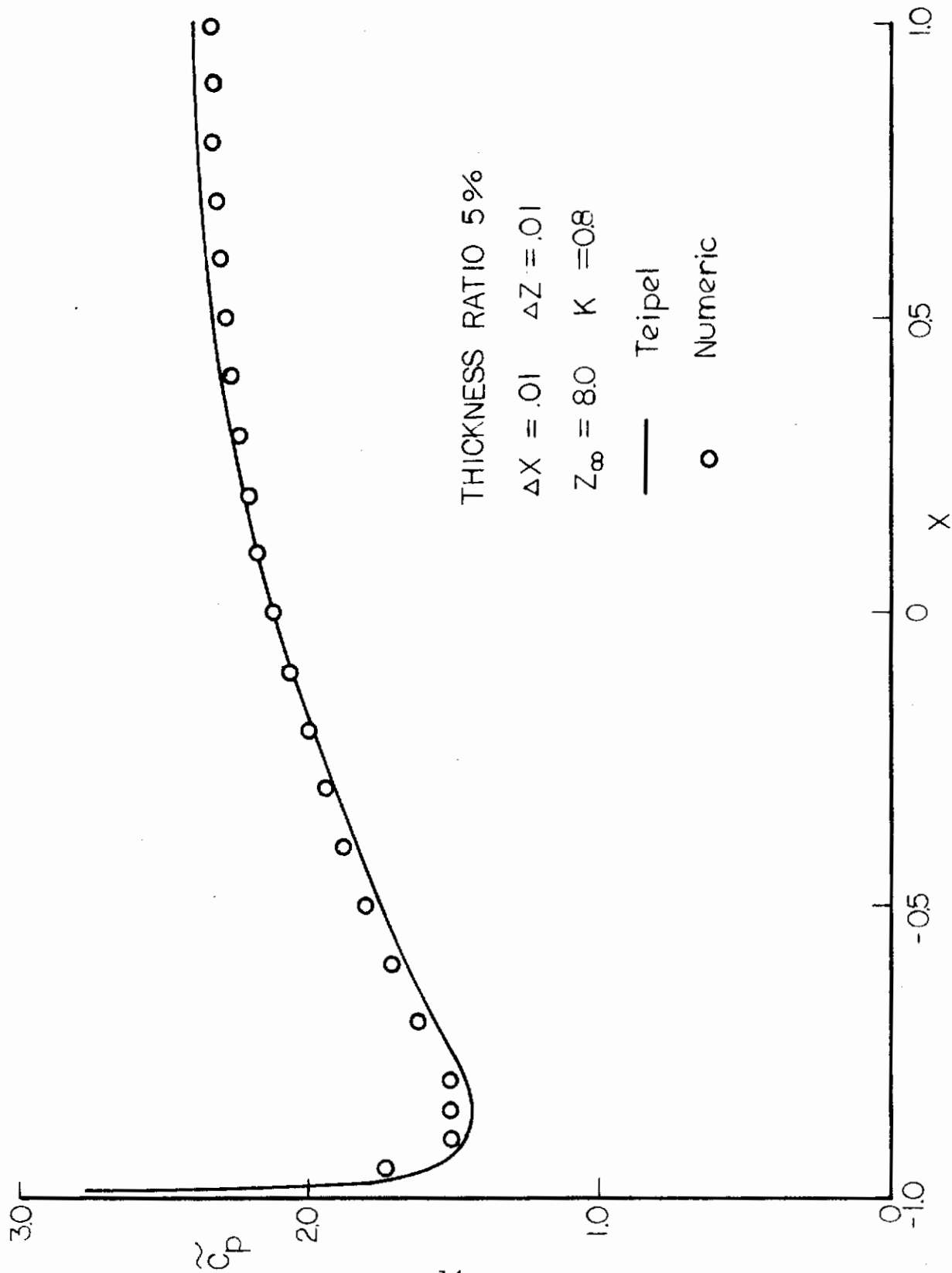


Figure 2. Real part of unsteady pressure coefficient for pitching wing.

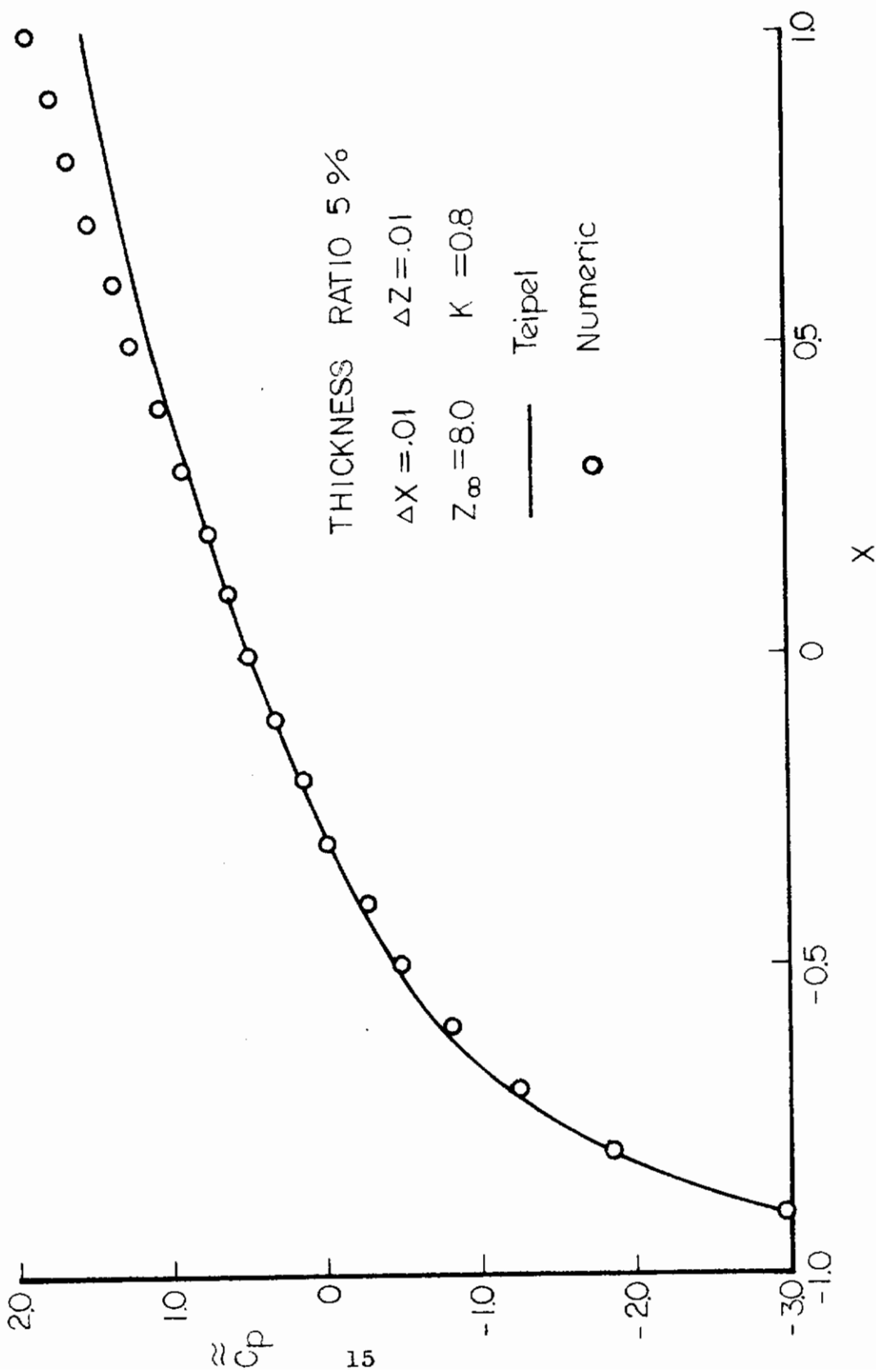


Figure 3. Imaginary part of unsteady pressure coefficient for pitching wing.



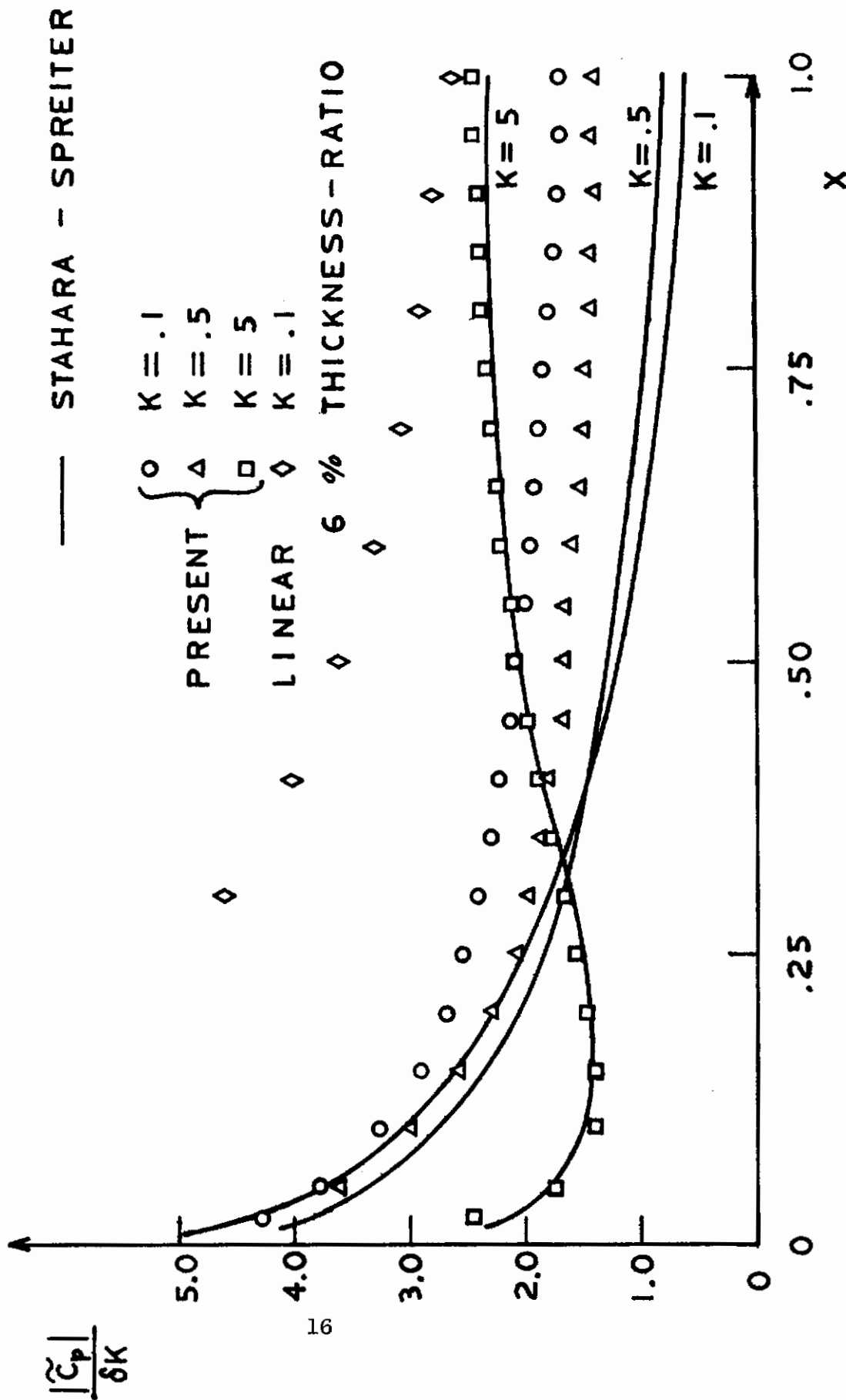
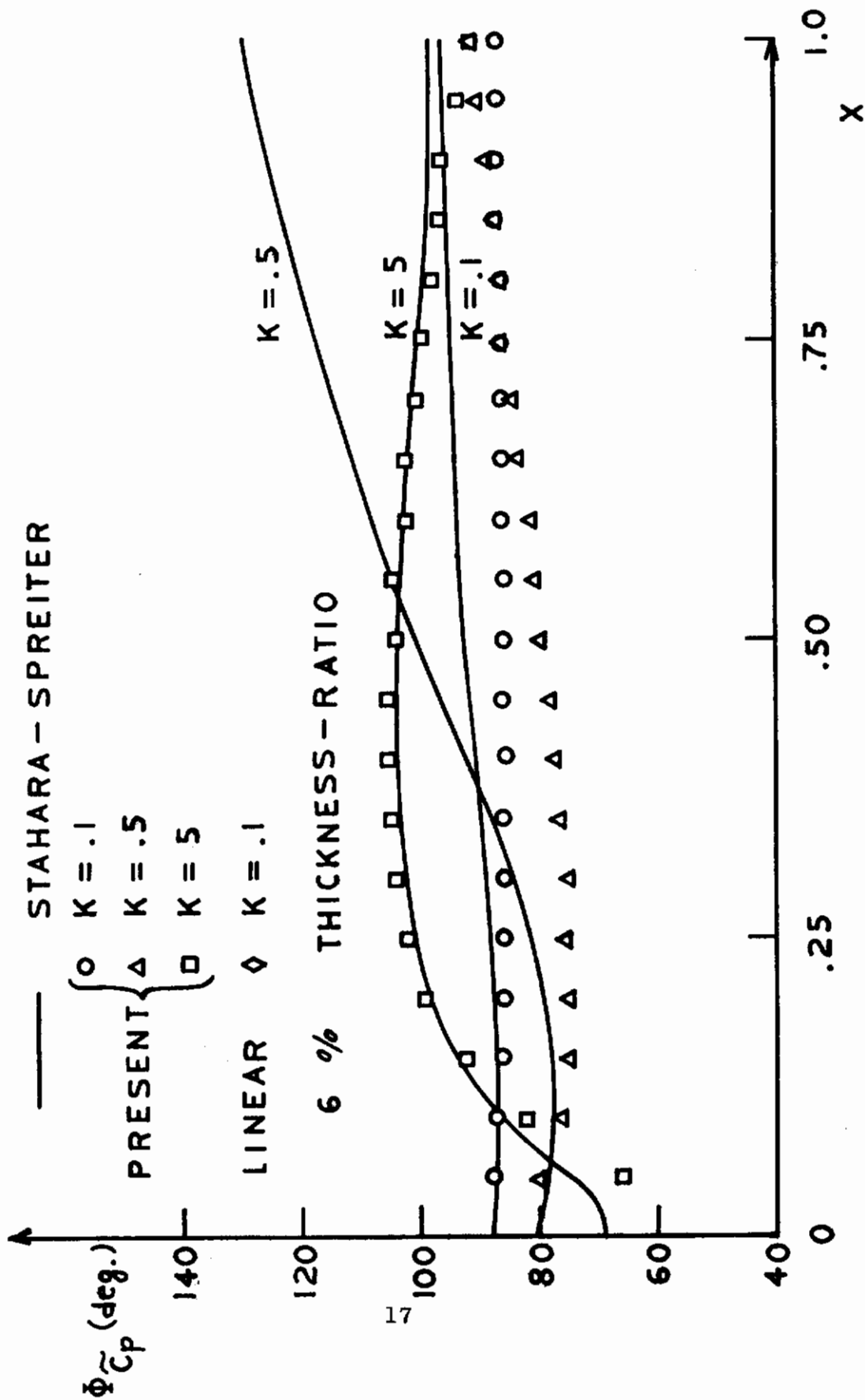


Figure 4. Magnitude of unsteady pressure distribution on 6% parabolic arc airfoil oscillating in plunge at  $M_\infty = 1$ .





17

Figure 5. Phase of unsteady pressure distributions on 6% parabolic arc airfoil oscillating in plunge at  $M_\infty = 1$ .

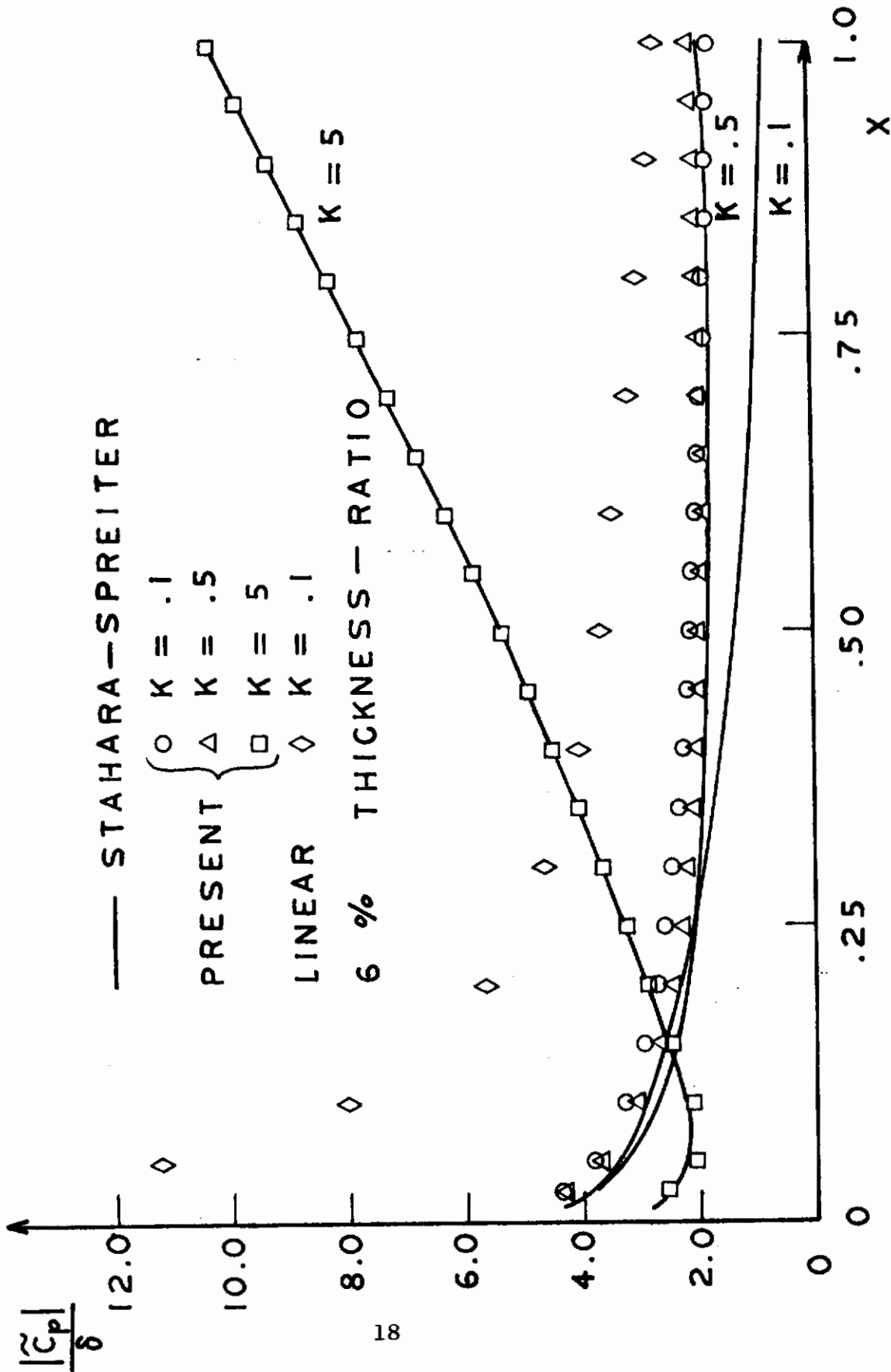


Figure 6. Magnitude of unsteady pressure distributions on 6% parabolic arc airfoil pitching about the nose at  $M_\infty = 1$ .

STAHARA - SPREITER

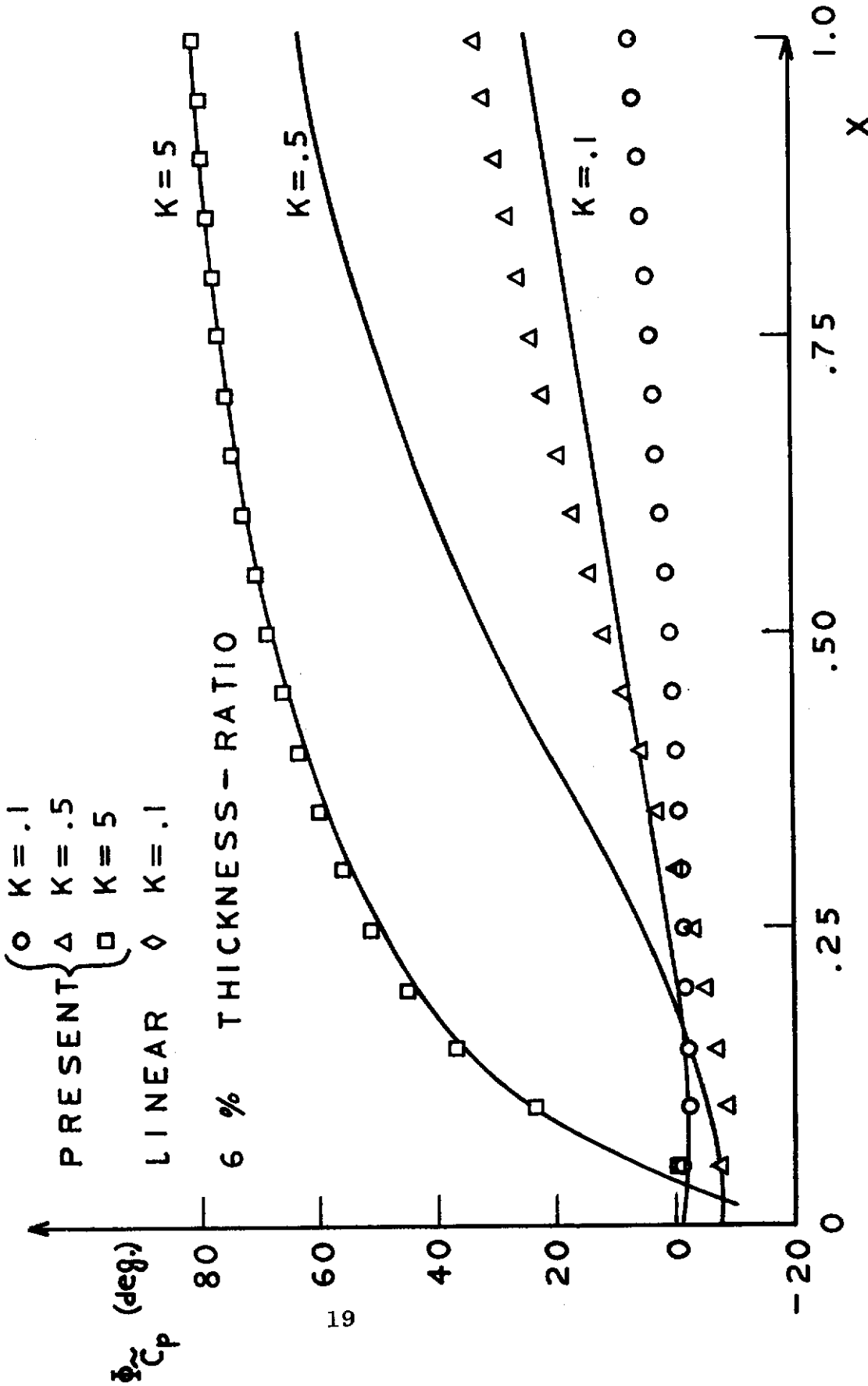


Figure 7. Phase of unsteady pressure distributions on 6% parabolic arc airfoil pitching about the nose at  $M_{\infty} = 1$ .

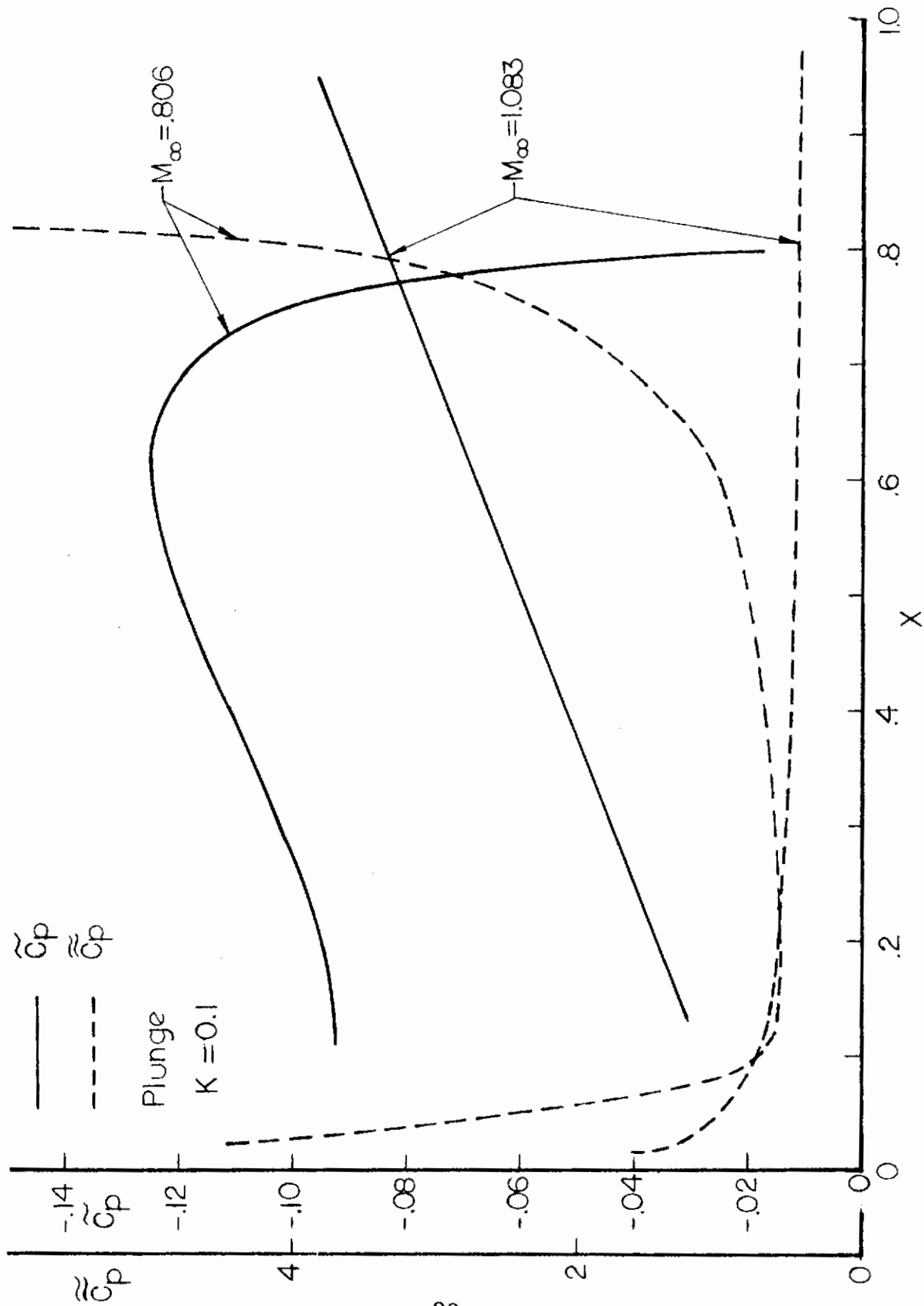


Figure 8. 6% Parabolic airfoil oscillating in plunge.

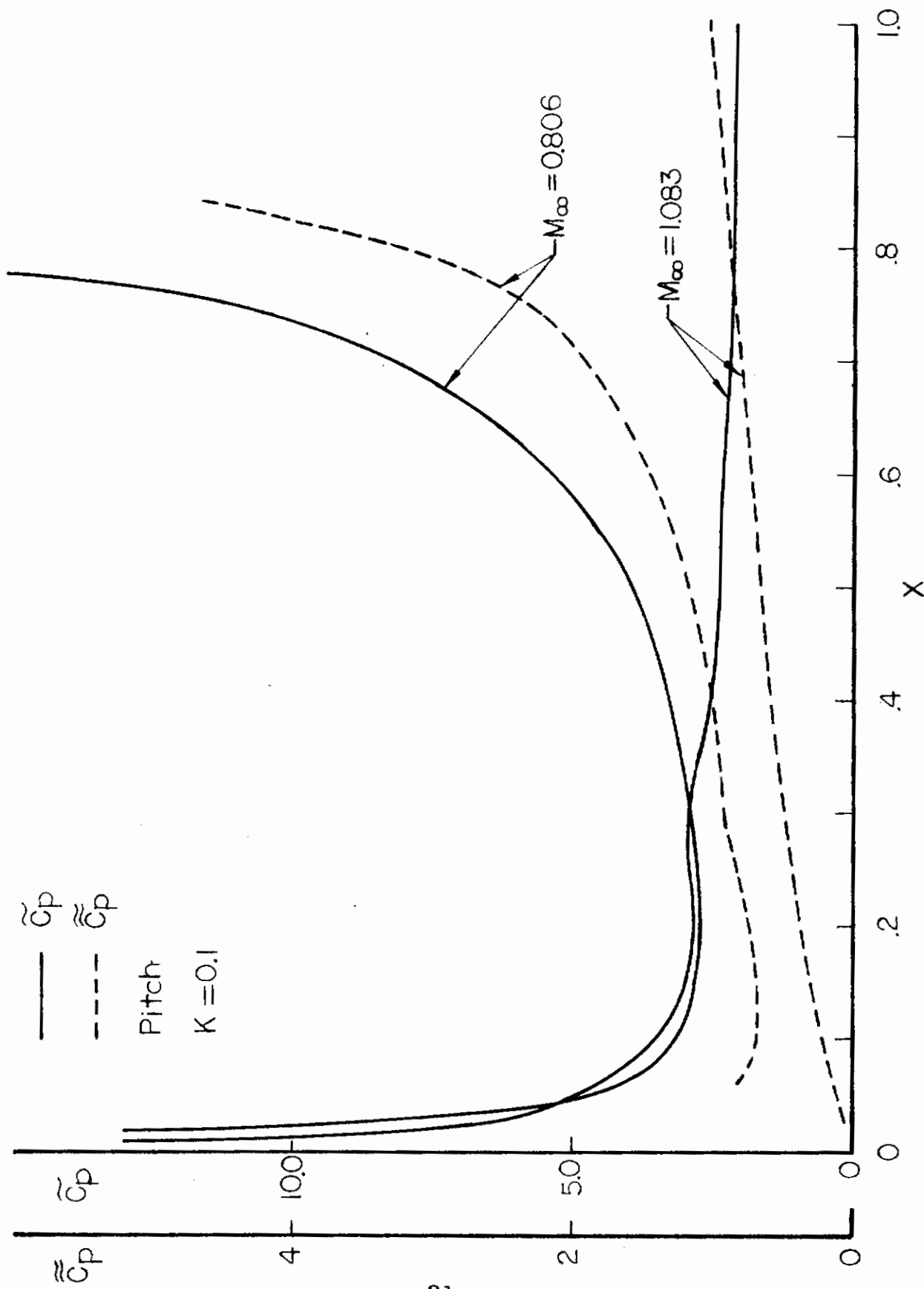


Figure 9. 6% Parabolic airfoil pitching about the nose.

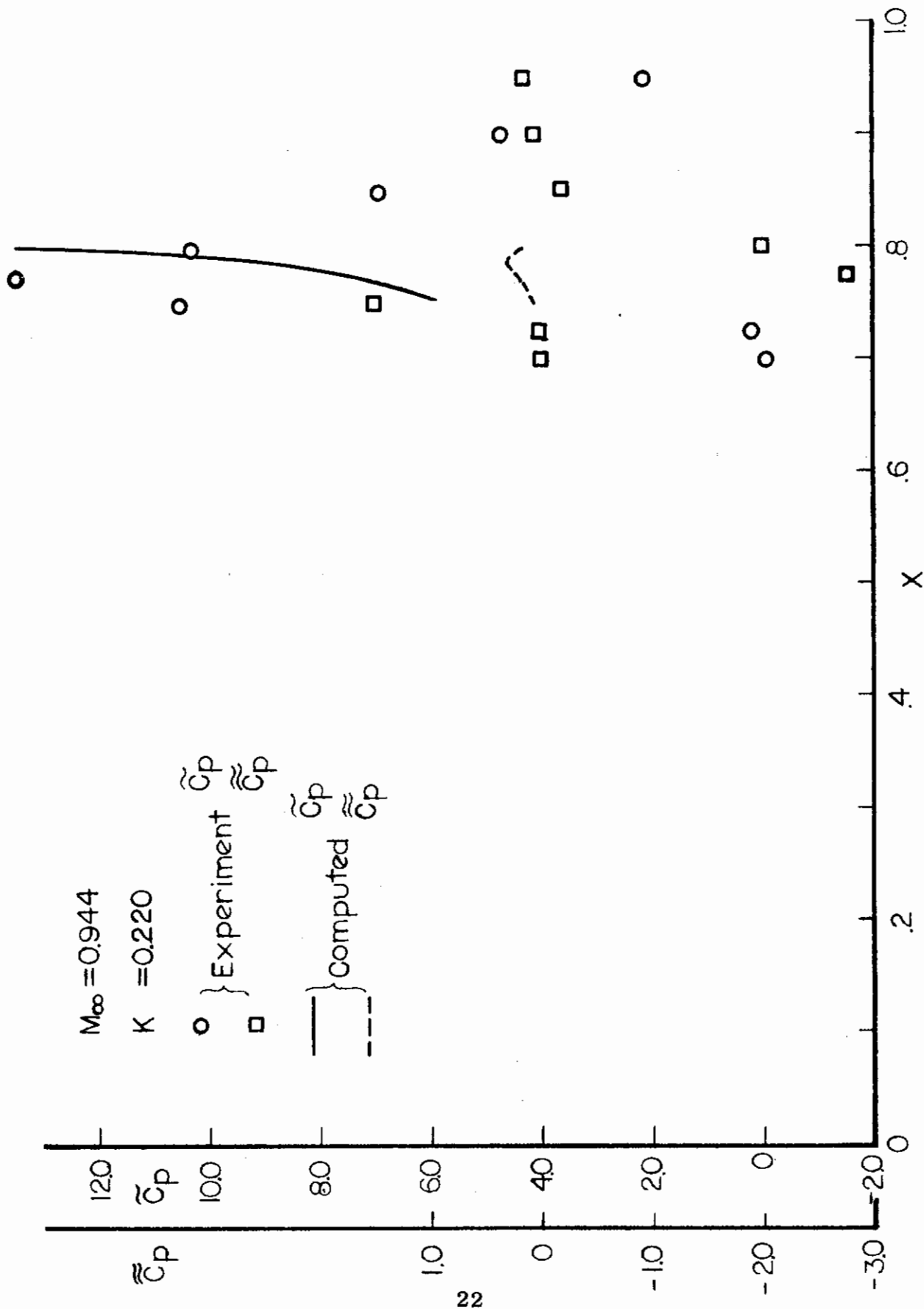


Figure 10. Oscillating control surface for  $M_\infty = .944$  at reduced frequency  $k = .220$ .

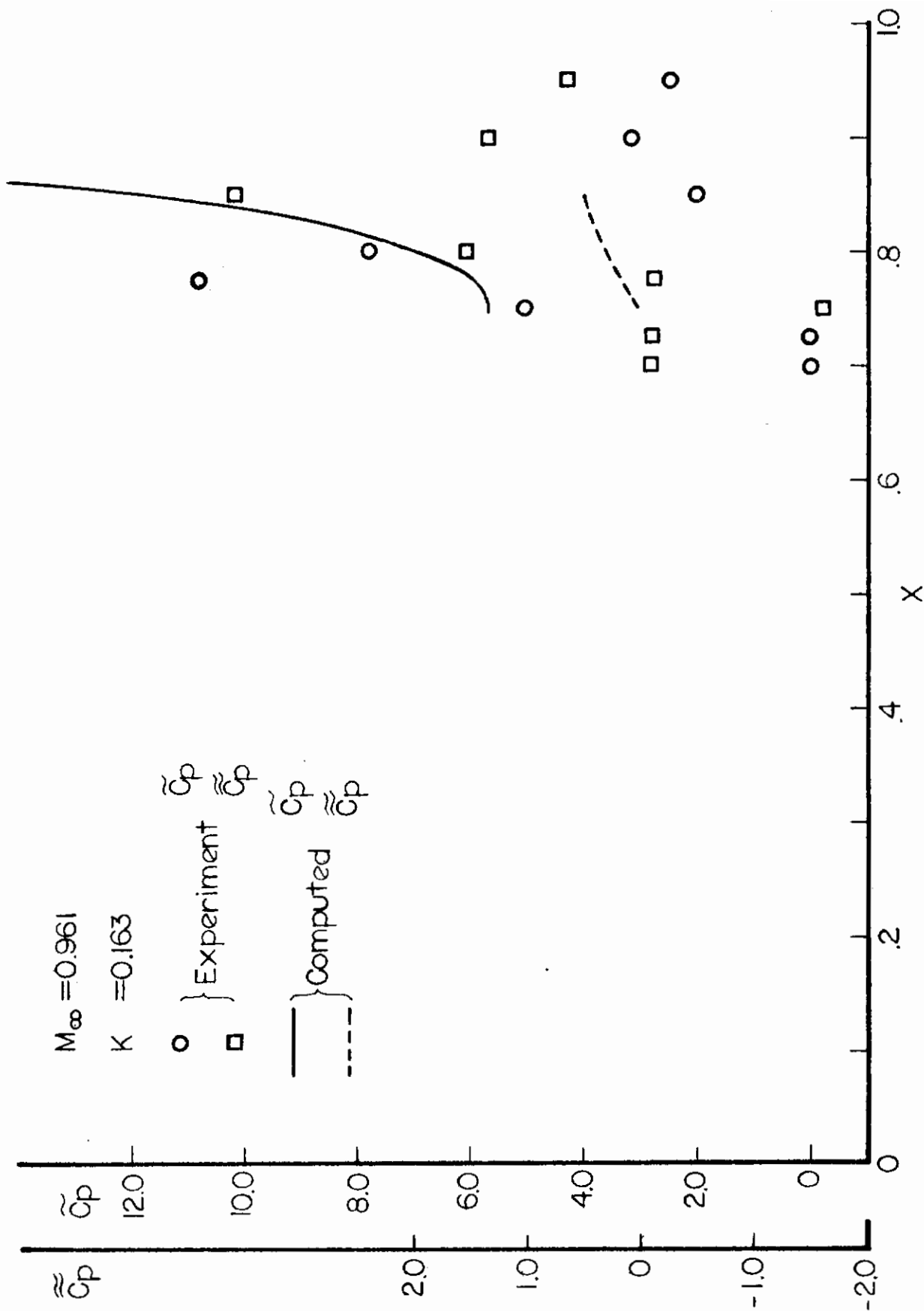


Figure 11. Oscillating control surface for  $M_\infty = .961$  at reduced frequency  $k = .163$ .

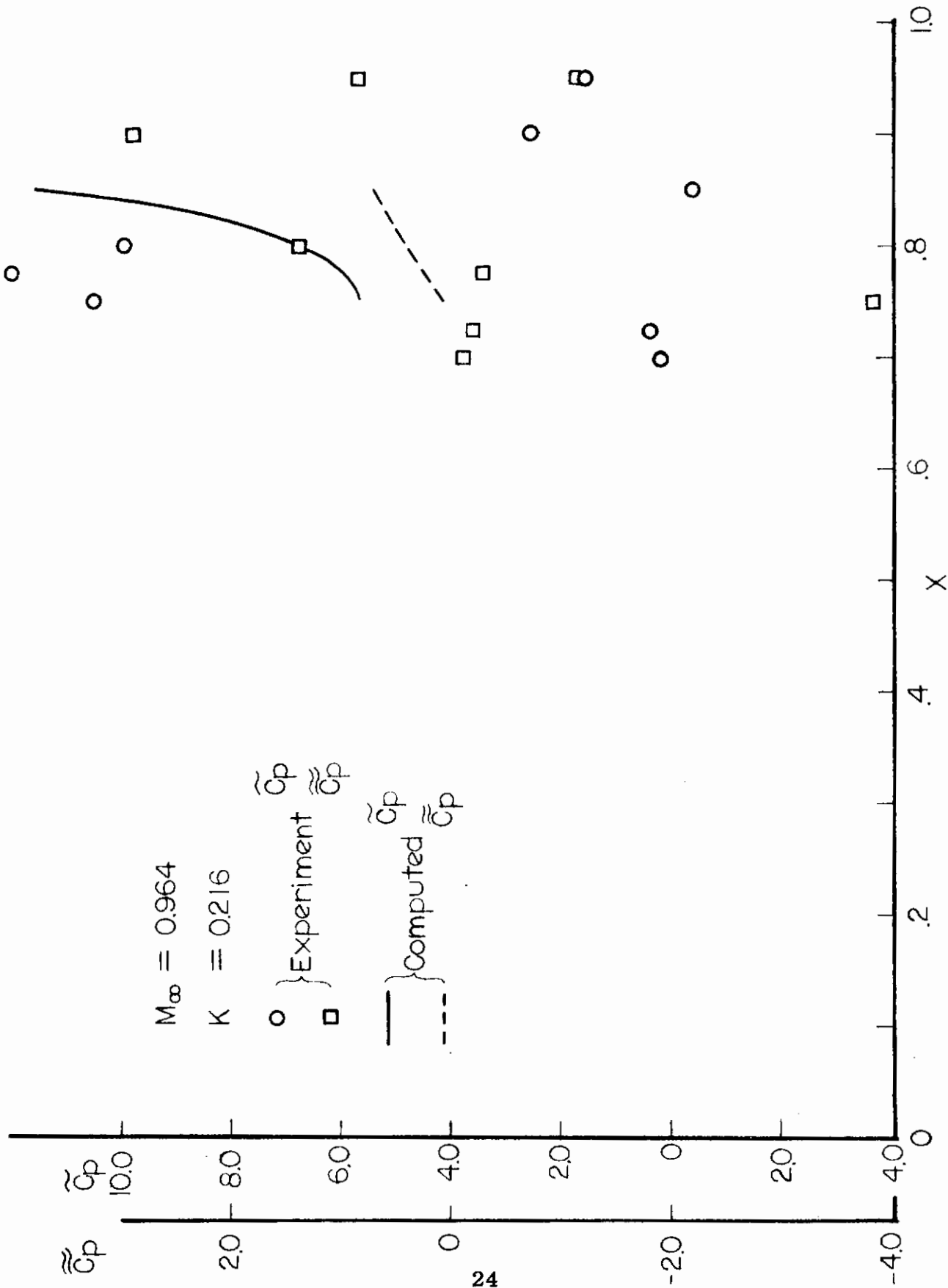


Figure 12. Oscillating control surface for  $M_\infty = .964$  at reduced frequency  $k = .216$ .



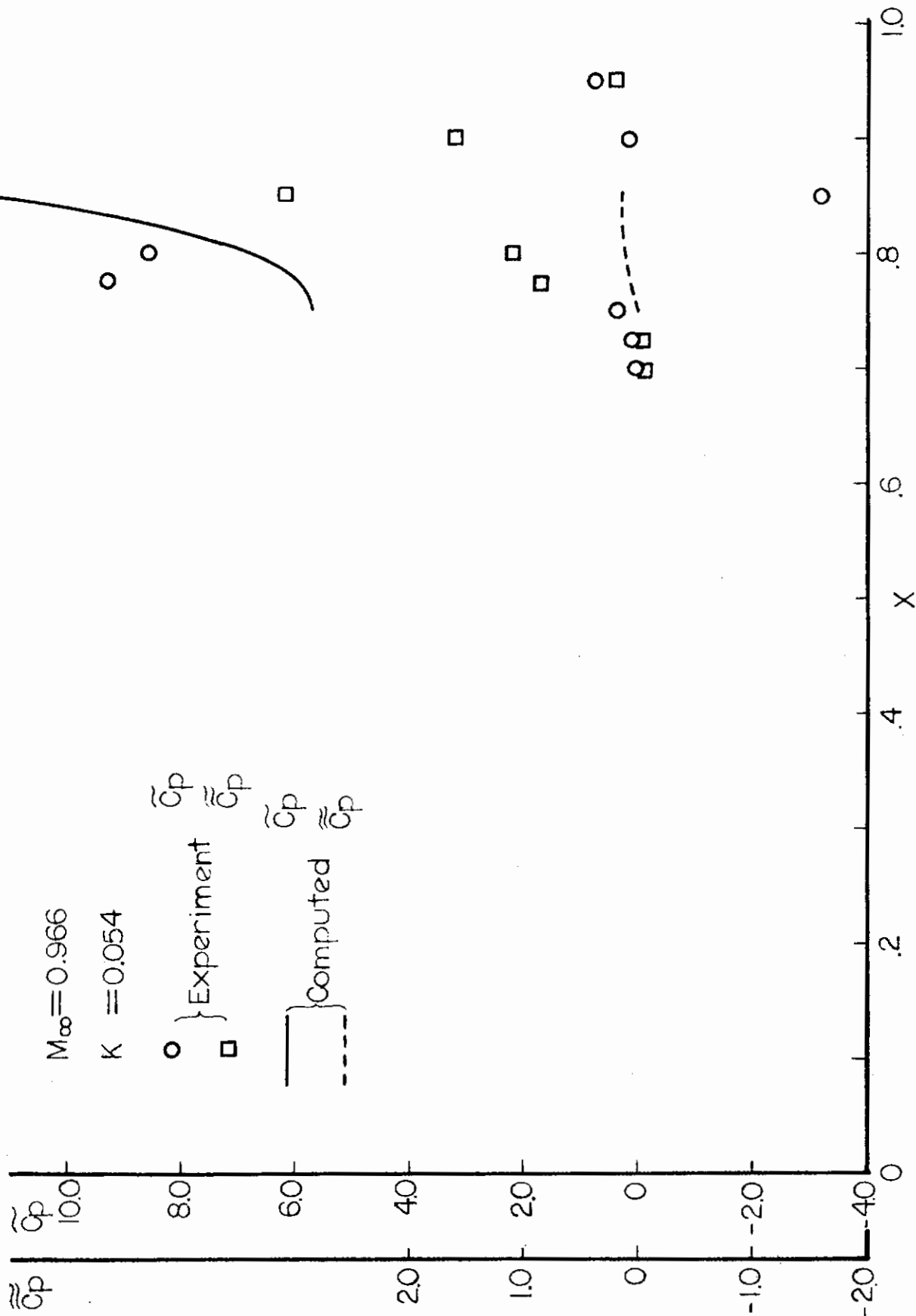


Figure 13. Oscillating control surface for  $M_\infty = .966$  at reduced frequency  $k = .054$ .

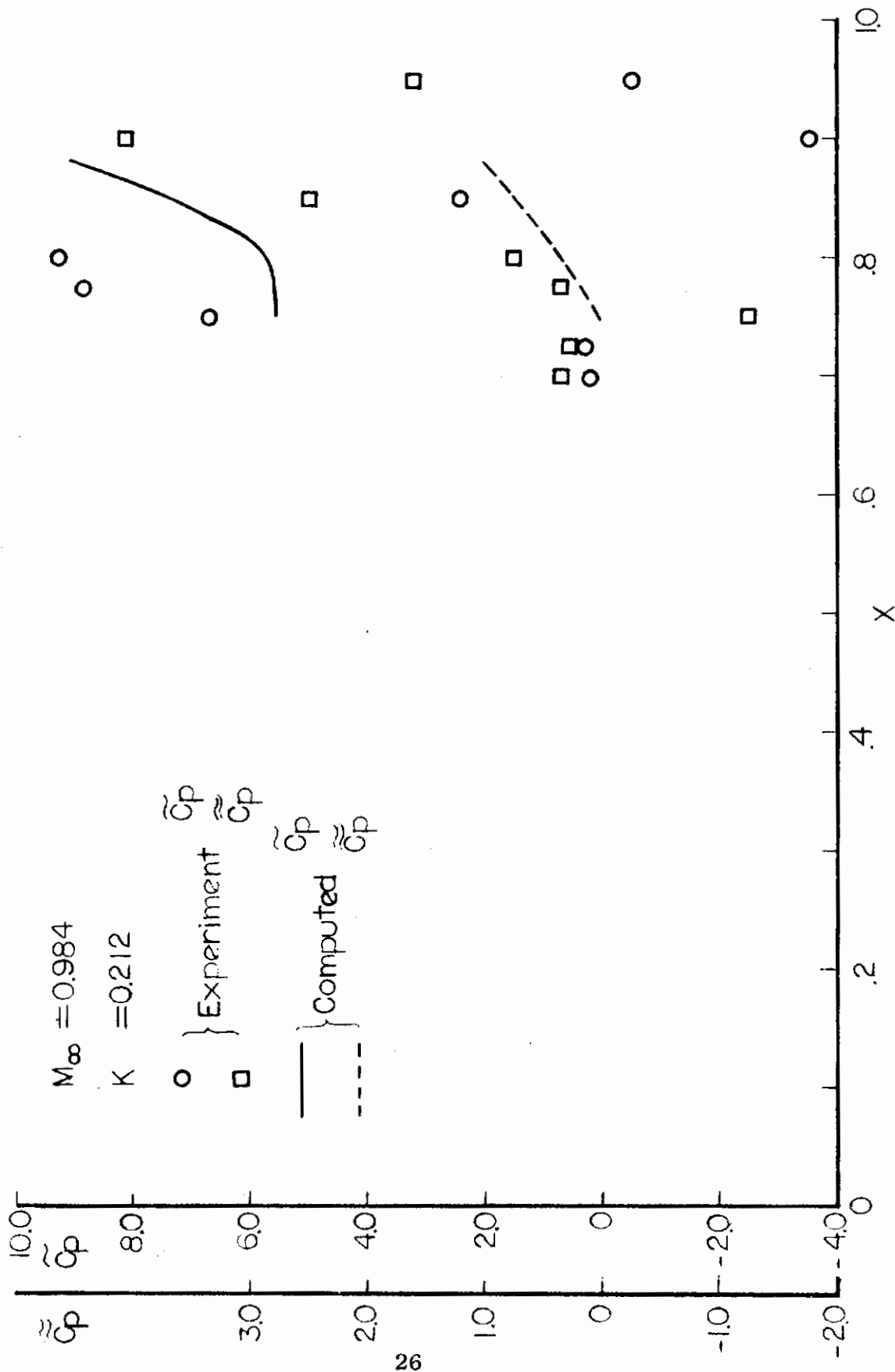


Figure 14. Oscillating control surface for  $M_\infty = .984$  at reduced frequency  $k = .212$ .

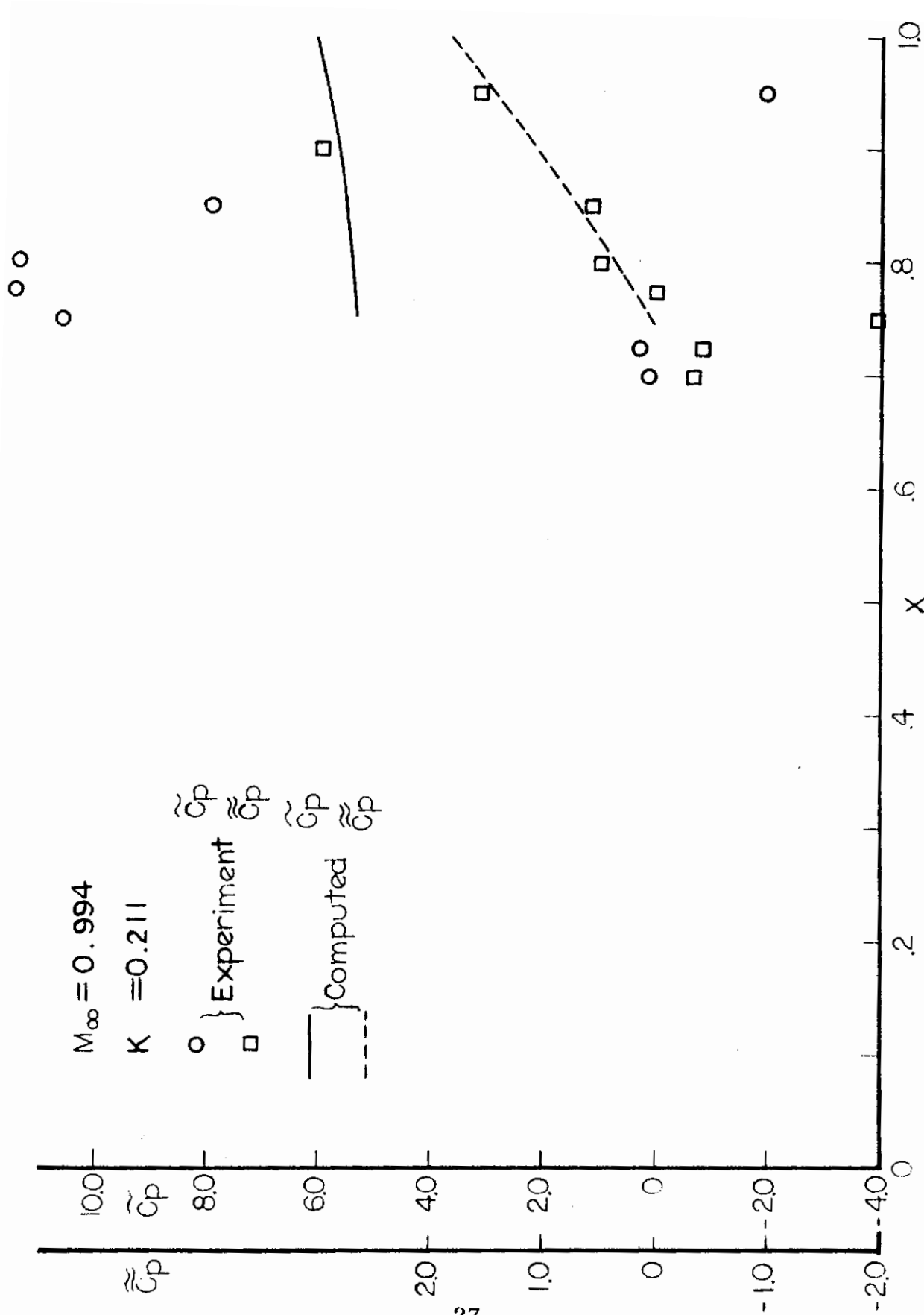


Figure 15. Oscillating control surface for  $M_\infty = .994$  at reduced frequency  $k = .211$ .

## REFERENCES

1. Liepmann, H. W. and Puckett, A. E., Aerodynamics of a Compressible Fluid, John Wiley and Sons, 1947, p. 45.
2. Wu, Jain-Ming and Aoyama, Kinya, "Preliminary Review of Approximate Calculative Methods for Transonic Flow Around Bodies of Revolution," Report No. RD-TR-72-4, U. S. Army Missile Command, Redstone Arsenal, Alabama, 1972.
3. Murman, E. M. and Cole, J. D., "Calculation of Plane Steady Transonic Flows," AIAA Journal, Vol. 9, No. 1, January 1971, pp. 114-121.
4. Bailey, F. R. and Steger, J. L., "Relaxation Techniques for Three-Dimensional Transonic Flow About Wings," AIAA Paper No. 72-189, presented at AIAA 10th Aerospace Sciences Meeting, San Diego, California, 17-19 January 1972.
5. Cunningham, Atlee M., Jr., "The Application of General Aerodynamic Lifting Surface Elements to Problems in Unsteady Transonic Flow," NASA CR-112264, February 1973.
6. Landahl, M. T., Unsteady Transonic Flow, Pergamon Press, New York, 1961.
7. Liu, D. D., Platzler, M. F., and Ruo, S. Y., "On the Calculation of Static and Dynamic Stability of Derivatives for Bodies of Revolution at Subsonic and Transonic Speeds," AIAA Paper No. 70-190, presented at AIAA Eighth Aerospace Sciences Meeting, New York, 19-21 January 1970.
8. Kimble, K. R., Liu, D. Y., Ruo, S. Y., and Wu, J. M., "Unsteady Transonic Flow Analysis for Low Aspect Ratio, Pointed Wings," AIAA Paper No. 73-122, presented at AIAA 11th Aerospace Sciences Meeting, Washington, D.C., 10-12 January 1973.
9. Teipel, I., "Die Instationaren Luftkrafte bei der Machzahl," Z. Flugwiss., 12, Heft 1, 1964; also, "The Nonsteady Aerodynamic Forces at Mach Number One," Translation RSIC-808, Redstone Arsenal, Alabama.
10. Tijdeman, H. and Bergh, H., "Analysis of Pressure Distributions Measured on a Wing with Oscillating Control Surface in Two-Dimensional High Subsonic and Transonic Flow," NLR-TR F. 253, March 1967.
11. Oswatitsch, K. and Keune, F., "Flow Around Bodies of Revolution at Mach Number One," paper presented at the Brooklyn Polytechnic Conference on High-Speed Aeronautics, 20-22 January 1955.

# Contrails

12. Cole, J. D. and Royce, W. W., "An Approximate Theory for the Pressure Distribution and Wave Drag of Bodies of Revolution at Mach Number One," Proceedings of the 6th Midwestern Conference on Fluid Mechanics, 1959.
13. Spreiter, J., "On the Application of Transonic Similarity Rules to Wings of Finite Span," TR 1153, National Advisory Committee for Aeronautics, 1953.
14. Hosokawa, I., "A Refinement of the Linearized Transonic Flow Theory," J. Phys. Soc. Japan, Vol. 15, No. 11, 1960, pp. 149-157.
15. Zierep, J., "Der Aquivalenzsatz und die Parabolische Methode fur Schallnahe Stromungen," Zamm 45, Heft 1, 1965, Seite 19-27.
16. Platzer, M. F. and Hoffman, G. H., "Quasi-Slender Body Theory for Slowly Oscillating Bodies of Revolution in Supersonic Flow," NASA TN D-3440, June 1966.
17. Ruo, S. Y. and Liu, D. D., "Calculation of Stability Derivatives for Slowly Oscillating Bodies of Revolution at Mach 1.0," Contract NAS8-20082, February 1971.
18. Stahara, Stephen S. and Spreiter, John R., "Development of a Nonlinear Unsteady Transonic Flow Theory," NASA CR-2258, June 1973.
19. Tijdeman, H. and Schippers, P., "Results of Pressure Measurements on an Airfoil with Oscillating Flap in Two-Dimensional High Subsonic and Transonic Flow (Zero Incidence and Zero Mean Flap Position)," NLR TR 73078 U, July 1973.
20. Estabrooks, B. B., "Wall-Interference Effects on Axisymmetric Bodies in Transonic Wind Tunnels," AEDC-TR-59-12, 1959.
21. Knechtel, Earl D., "Experimental Investigation at Transonic Speeds of Pressure Distributions Over Wedge and Circular-Arc Airfoil Sections and Evaluation of Perforated-Wall Interference," NASA TN D-15, August 1959.

# *Contrails*

UNCLASSIFIED

Security Classification

DOCUMENT CONTROL DATA - R & D		
<i>(Security classification of title, body of abstract and indexing annotation must be entered when the overall report is classified)</i>		
1. ORIGINATING ACTIVITY (Corporate author) The University of Tennessee Space Institute Tullahoma, Tennessee 37388		2a. REPORT SECURITY CLASSIFICATION Unclassified
		2b. GROUP N/A
3. REPORT TITLE AN APPROXIMATE SOLUTION OF UNSTEADY TRANSONIC FLOW PROBLEMS		
4. DESCRIPTIVE NOTES (Type of report and inclusive dates) June 1973 to January 1974		
5. AUTHOR(S) (First name, middle initial, last name) J. M. Wu, K. R. Kimble		
6. REPORT DATE June 1974	7a. TOTAL NO. OF PAGES 29	7b. NO. OF REFS 21
8a. CONTRACT OR GRANT NO. F 33615-73-C-3119	9a. ORIGINATOR'S REPORT NUMBER(S) AFFDL-TR-74-32	
b. PROJECT NO. 1929	9b. OTHER REPORT NO(S) (Any other numbers that may be assigned this report)	
c. Task No. 192905	N/A	
d.		
10. DISTRIBUTION STATEMENT Approved for public release; distribution unlimited.		
11. SUPPLEMENTARY NOTES		12. SPONSORING MILITARY ACTIVITY Air Force Flight Dynamics Laboratory Wright-Patterson A.F.B., Ohio 45433
13. ABSTRACT Unsteady pressures on a thin two-dimensional airfoil pitching and plunging in transonic flow have been computed by numerically solving the governing partial differential equation. The effect of wing thickness has been retained by using the steady flow potential on the wing in the coefficients of the equation in a manner which generalizes Oswatitsch's parabolic method. The results are compared with other methods and with experimental data.		

DD FORM 1 NOV 65 1473

UNCLASSIFIED

Security Classification

Security Classification

14. KEY WORDS	LINK A		LINK B		LINK C	
	ROLE	WT	ROLE	WT	ROLE	WT
Unsteady Transonic Flow Parabolic Method Local Linearization Oscillatory Aerodynamics Numerical Solutions						

UNCLASSIFIED

Security Classification

★U.S. Government Printing Office: 1974 - 758-436/723